

## Effects of Radiation and Chemical Reaction on MHD Convective Flow over a Permeable Stretching Surface with Suction and Heat Generation

Penem Mohan KRISHNA<sup>1</sup>, Naramgari SANDEEP<sup>2</sup> and Vangala SUGUNAMMA<sup>3,\*</sup>

<sup>1</sup>Research Scholar, Department of Mathematics, Sri Venkateswara University, Tirupati, India

<sup>2</sup>Division of Fluid Dynamics, Vellore Institute of Technology University, Vellore, India

<sup>3</sup>Department of Mathematics, Sri Venkateswara University, Tirupati, India

(\*Corresponding author's e-mail: vsugunar@yahoo.co.in)

Received: 6 December 2013, Revised: 5 February 2014, Accepted: 6 March 2014

### Abstract

In this study, we analyze the effects of thermal radiation and chemical reaction on the steady 2 dimensional stagnation point flow of a viscous incompressible electrically conducting fluid over a stretching surface, with suction and heat generation. The partial differential equations governing the flow are solved numerically by using the shooting technique. The effects of various parameters on velocity, temperature, and concentration profiles, as well as Nusselt number, Skin friction coefficient, and Sherwood number, are examined, and presented graphically and through tables. It is found that velocity, temperature, and rate of heat transfer of the fluid are influenced more by radiation and chemical reaction parameters, along with applied magnetic field.

**Keywords:** Thermal radiation, MHD, convection, chemical reaction, heat generation

### Introduction

Flow of an incompressible viscous fluid over a stretching surface has important applications in the polymer industry. Recently, Sandeep and Sugunamma [1] analyzed the unsteady free convective flow through a porous medium past a vertical plate in the presence of a magnetic field with constant heat generation. The study of a viscous fluid flow due to a stretching surface is an important type of flow, occurring in several engineering processes. Such processes include wire drawing, heat-treated materials travelling between a feed roll and a wind-up roll or materials manufactured by extrusion, glass-fiber and paper production, cooling of metallic sheets or electronic chips, crystal growing, drawing of plastic sheets, and many others. In these cases, the desired characteristics the final product depends on the rate of cooling in the process and the process of stretching. All of the above investigations were restricted to flows of Newtonian fluids; of late, non-Newtonian fluids have become more and more important industrially. The boundary layer flow caused by a continuously stretching sheet is often encountered in many engineering and industrial processes. Such flows are of interest in the manufacture of sheeting material through an extrusion process. Gupta and Gupta [2] have analyzed heat and mass transfer in a stretching problem with a constant surface temperature, while Soundalgekar and Rheol [3] investigated the Stokes problem for a viscoelastic fluid. Sugunamma *et al.* [4] discussed the radiation effects due to natural convection flow between heated inclined plates under the influence of transverse magnetic field, and they concluded that fluid flow is influenced more by magnetic field effect. Sandeep [5] investigated the magnetic field effects between heated inclined plates due to natural convection in the presence of a heat source. Rao *et al.* [6] studied arbitrary injection/suction at a moving wall in a power-law fluid. Crane [7] extended the problem of Sakiadis [8,9] to that of a stretching sheet whose velocity is proportional to

the distance from the slit. This type of flow usually occurs in the drawing of plastic films and artificial fibers. Chen and Char [10] investigated the heat transfer characteristics over a continuous stretching surface with a variable surface temperature. Temperature distribution in the flow over a stretching surface subject to uniform heat flux was studied by Dutta *et al.* [11]. Bhattacharyya *et al.* [12] studied the temperature distribution in the steady boundary layer flow of a second-order fluid past a stretching surface. Such fluids are referred to as fluids of differential type, or informally as Rivlin-Erickson fluids [13]. These fluids show viscoelastic behavior in so far as in flows of such fluids. Flow of an incompressible viscous fluid over a stretching sheet has an important bearing on several technological processes. In particular, in the extrusion of a polymer in a melt-spinning process, the extrudate from the die is generally drawn and simultaneously stretched into a sheet, which is then solidified through quenching or gradual cooling by direct contact with water. Further glass blowing, continuous casting of metals, and spinning of fibers involve the flow due to a stretching surface. In all of these cases, the quality of the final product depends on the rate of heat transfer at the stretching surface. Bujurke *et al.* [14] studied the heat transfer in the flow of a second order fluid over a stretching sheet with a constant surface temperature. Sugunamma *et al.* [15] analyzed the inclined magnetic field and chemical reaction effects on the flow on the semi infinite vertical porous plate through a porous medium. Sandeep and Sugunamma [16] investigated the laminar convective flow of a dusty viscous fluid in the presence of magnetic field and heat source. A systematic study of the steady 2-dimensional stagnation point flow of an upper-convected Maxwell fluid was provided by Hayat *et al.* [17]. Most boundary-layer models can be reduced to systems of nonlinear ordinary differential equations, which are usually solved by numerical methods. Analytical methods have significant advantages over numerical methods in providing analytic, verifiable, rapidly convergent approximation. Andersson and Dandapat [18] investigated the steady 2 dimensional non-Newtonian flow of a power-law fluid past a stretching surface. Siddappa and Abel [19] considered the non-Newtonian flow past a stretching plate and obtained the solution of motion equations. Char and Chen [20] investigated the heat transfer in a viscoelastic fluid of waters liquid B model over a stretching plate subject to a power-law heat flux. However, all of the above research dealing with the non-Newtonian fluids concentrated only on the heat transfer problems. None of them dealt with the much more complicated problem involving both the heat and the mass transfer in the electrically conducting fluid.

To the author's knowledge, no studies have been communicated so far with regard to the radiation and chemical reaction on MHD convective flow over a permeable stretching surface with suction and heat generation by using the shooting technique. The present study is of immediate application to all those processes which are highly affected by the heat enhancement concept. It is pertinent to mention here that some researchers have pursued their investigations with heat source, but the effects of radiation and chemical reaction on MHD convective flow over a permeable stretching surface with suction and heat generation is presented in this paper clearly.

### Mathematical analysis

We consider the steady 2 dimensional stagnation point flow of a viscous incompressible electrically conducting fluid near a stagnation point at a surface coinciding with the plane  $y = 0$ , with the flow being restricted to  $y > 0$ . Two equal and opposing forces are applied along the  $x$ -axis so that the surface is stretched (while keeping the origin fixed). The potential flow that arrives from the  $y$ -axis (impinging on the flat wall at  $y = 0$ ) divides into 2 streams on the wall and leaves in both directions. The flow is through a porous medium where the Darcy model is assumed. The viscous flow must adhere to the wall, whereas the potential flow slides along it. We denote the components of the fluid velocity by  $(u, v)$  at any point  $(x, y)$  for the viscous flow, while  $(U, V)$  denote the velocity components for the potential flow. We consider the case in which there may be a suction velocity  $(-W)$  on the stretching surface. Also, we denote the fluid temperature by  $T$ . The velocity distribution of the frictionless flow in the neighborhood of the stagnation point becomes;

$$U(x) = ax, \quad V(x) = -ay \quad (1)$$

where the parameter  $a > 0$  is proportional to the free stream velocity. The continuity and momentum equations for the two dimensional steady flow using the usual boundary layer approximation reduces to:

#### Continuity equation

$$\frac{\partial u}{\partial x} + \frac{\partial v}{\partial y} = 0 \quad (2)$$

#### Momentum equation

$$\rho \left( u \frac{\partial u}{\partial x} + v \frac{\partial u}{\partial y} \right) = -\frac{\partial p}{\partial x} + \mu \frac{\partial^2 u}{\partial y^2} + g\beta\rho(T - T_\infty) + g\beta^*\rho(C - C_\infty) + \sigma B_0^2 u + \frac{\mu}{k'} u \quad (3)$$

where

$$-\frac{\partial p}{\partial x} = U \frac{dU}{dx} + \frac{\sigma B_0^2}{\rho} U + \frac{\nu}{k'} U \quad (4)$$

#### Energy equation

$$\rho c_p \left( u \frac{\partial T}{\partial x} + v \frac{\partial T}{\partial y} \right) = k \frac{\partial^2 T}{\partial y^2} + Q(T - T_\infty) - \frac{\partial q_r}{\partial y} \quad (5)$$

#### Species diffusion equation

$$u \frac{\partial C}{\partial x} + v \frac{\partial C}{\partial y} = D \frac{\partial^2 C}{\partial y^2} - K_l'(C - C_\infty) \quad (6)$$

On substituting the Eq. (4) in Eq. (3), we get;

$$\rho \left( u \frac{\partial u}{\partial x} + v \frac{\partial u}{\partial y} \right) = U \frac{dU}{dx} + \mu \frac{\partial^2 u}{\partial y^2} + g\beta\rho(T - T_\infty) + g\beta^*\rho(C - C_\infty) + \sigma B_0^2 (U - u) + \frac{\mu}{k'} (U - u) \quad (7)$$

where  $u$  and  $v$  are the velocity components along the X and Y axes respectively.  $\mu$  is the coefficient of viscosity of the fluid.  $\nu$  is the kinematic viscosity.  $\beta$  and  $\beta^*$  are the thermal and concentration expansion coefficient, respectively.  $\sigma$  is the electrical conductivity.  $B_0$  is the uniform magnetic field.  $\rho$  is the density.  $T$  is the temperature inside the boundary layer.  $T_\infty$  is the temperature far away from the plate.  $C$  is the species concentration in the boundary layer.  $C_\infty$  is the species concentration of an ambient fluid.  $C_p$  is the specific heat at constant pressure.  $k$  is the thermal conductivity.  $k'$  is the porosity parameter.  $Q$  is the volumetric rate of heat generation.  $D$  is the molecular diffusivity of the species

concentration.  $K_l'$  is the Chemical reaction parameter and  $K_l$  is dimensionless chemical reaction parameter.

The corresponding boundary conditions are;

$$\begin{aligned} u = cx, v = 0, T = T_w, C = C_w \text{ at } y = 0 \\ u = ax, T \rightarrow T_\infty, C \rightarrow C_\infty \text{ as } y \rightarrow \infty \end{aligned} \quad (8)$$

where  $c > 0$ .

By using Roseland approximation, the radiative heat flux  $q_r$  is given by  $q_r = -\frac{4\sigma^*}{3k^*} \frac{\partial T^4}{\partial y}$  where  $\sigma^*$  is the Steffen Boltzmann constant and  $k^*$  is the mean absorption coefficient. Considering the temperature differences within the flow to be sufficiently small, such that  $T^4$  may be expressed as the linear function of temperature, then expanding  $T^4$  in Taylor series about  $T_\infty$  and neglecting higher-order terms, we get  $T^4 \cong 4T_\infty^3 T - 3T_\infty^4$ .

We introduce the following non-dimensional variables;

$$\begin{aligned} M = \frac{\sigma B_0^2}{\rho c}, H = \frac{Q}{c \rho c_p}, Pr = \frac{\mu c_p}{k}, K = \frac{\nu}{ck'}, Sc = \frac{\nu}{D}, \\ s = \frac{W}{\sqrt{c\nu}}, Gr = \frac{g\beta(T_w - T_\infty)}{xc^2}, Gc = \frac{g\beta^*(C_w - C_\infty)}{xc^2}, \\ \theta = \frac{T - T_\infty}{T_w - T_\infty}, \phi = \frac{C - C_\infty}{C_w - C_\infty}, R = \frac{16T_\infty^3 \sigma^*}{3k^*}, K_l = \frac{K_l'}{c} \end{aligned} \quad (9)$$

$$\eta = \sqrt{\frac{c}{\nu}} y, \psi = \sqrt{c\nu} x f(\eta) \quad (10)$$

where  $F(\eta)$  is a dimensionless stream function.  $\theta(\eta)$  is a dimensionless temperature of the fluid in the boundary layer region.  $\phi(\eta)$  is a dimensionless species concentration of the fluid in the boundary layer region, and  $\eta$  is the similarity variable. The velocity components  $u$  and  $v$  are respectively obtained as follows;

$$u(x, y) = \frac{\partial \psi}{\partial y} = xcf'(\eta), \quad v(x, y) = -\frac{\partial \psi}{\partial x} = -\sqrt{c\nu} f(\eta) \quad (11)$$

In view of Eqs. (9), (10) and (11), Eqs. (5) to (7) take the forms as below;

$$f''' + ff'' - (f')^2 + Gr\theta + Gc\phi + (M + K)(C - f') + C^2 = 0 \quad (12)$$

$$(1 + R)\theta'' + \text{Pr}(f\theta' + H\theta) = 0 \quad (13)$$

$$\phi'' + \text{Sc}(f\phi' - K_1\phi) = 0 \quad (14)$$

where the primes denote the differentiation with respect to  $\eta$ .  $K$  is the Darcy permeability parameter.  $M$  is the magnetic parameter.  $C = a/c > 0$  is the stretching parameter.  $H$  is the heat source parameter.  $\text{Pr}$  is the Prandtl number.  $\text{Sc}$  is the Schmidt number.  $R$  is the radiative parameter.  $Gr$  is the Grashof number and  $GC$  is the modified Grashof number.

The corresponding boundary conditions are;

$$\begin{aligned} f' = 1, f = s, \theta = 1, \phi = 1 \quad \text{at} \quad \eta = 0 \\ f' = C, \theta = 0, \phi = 0 \quad \text{as} \quad \eta \rightarrow \infty \end{aligned} \quad (15)$$

### Solution of the problem

The governing boundary layers Eqs. (12) to (14), corresponding to velocity, temperature, and species concentration, subject to boundary condition (15), are solved numerically by using the shooting method. First of all, higher order non-linear differential Eqs. (12) to (14) are converted into simultaneous linear differential equations of the first order, and they are further transformed into initial value problem by applying the shooting technique. From the process of numerical computation, the skin-friction coefficient, the Nusselt number, and the Sherwood number, which are respectively proportional to  $f''(0)$ ,  $-\theta'(0)$  and  $-\phi'(0)$  are also sorted out, and their numerical values are presented in a tabular form.

The skin-friction and the rate of heat and mass transfer are the most important characteristics of the flow which are defined as:

The coefficient of skin-friction,

$$C_f = \frac{2\tau_w}{\rho U_\infty^2} = 2 \text{Re}^{-1/2} x^{-1/2} f''(0) \quad (16)$$

where  $\tau_w = \mu(\partial u/\partial y)_{y=0}$ ;

The coefficient of rate of heat transfer,

$$Nu = -\frac{xq_w}{k(T_w - T_\infty)} = -\text{Re}^{1/2} x^{1/2} \theta'(0) \quad (17)$$

where  $q_w = -k(\partial T/\partial y)_{y=0}$ ;

The coefficient of rate of mass transfer,

$$Sh = -\frac{xm_w}{D(C_w - C_\infty)} = -\text{Re}^{1/2} x^{1/2} \phi'(0) \quad (18)$$

where  $m_w = -D(\partial C/\partial y)_{y=0}$ .

### Results and discussion

In order to get a physical insight into the problem, the effects of various governing parameters on the physical quantities are computed and represented in **Figures 1 - 20** and discussed in detail.

The influence of  $M$  on velocity profiles has been illustrated in **Figure 1**. It is observed that, while all other participating parameters are held constant and  $M$  is increased, the velocity decreases in general. From **Figure 2**, it is noticed that the temperature of flow field is increased with the increase of  $M$ . The effect of  $M$  on concentration field is illustrated in **Figure 3**. It is observed that increase in  $M$  contributes to the increase of concentration of the fluid. The contribution of  $Gr$  on the velocity profiles is noticed in **Figure 4**. An increase in  $Gr$  shows the increase in the velocity field. The influence of  $Gr$  on the temperature and concentration profiles are illustrated in **Figures 5 and 6**. It is observed that an increase in  $Gr$  contributes to a decrease of temperature and concentration of the fluid medium respectively. The velocity and temperature profiles for different values of  $Pr$  are represented in **Figures 7 and 8**. The effect of  $Pr$  dominates in both velocity and temperature fields. It is observed that the velocity and temperature decreases with an increase of  $Pr$ . The influence of  $Pr$  on concentration profiles has been illustrated in **Figure 9**. It is observed that, while all other participating parameters are held constant and  $Pr$  is increased, the velocity increases in general. **Figures 10 and 11** illustrate the velocity and concentration profiles for different values of the  $Sc$ . The trend shows that the velocity and concentration decreases with an increase of  $Sc$ . **Figure 12** shows the effect of the  $Gc$  on velocity profiles. It is noticed that the velocity of flow field is increased as the values of  $Gc$  increased. **Figures 13 and 14** illustrate the effect of  $Gc$  on temperature and concentration profiles. It is observed that, while all other participating parameters are held constant and  $Gc$  is increased, the temperature and concentration decreases in general. **Figures 15 and 16** show the velocity and temperature profiles for different values of heat source parameter. It is clear that the velocity and temperature decreases with an increase of heat source parameter. The influence of radiation parameter on the velocity and temperature profiles is illustrated in **Figure 17 and 18**. It is observed that an increase in radiation parameter contributes to increase of both velocity and temperature of the fluid medium. The velocity and temperature profiles for different values of chemical reaction parameter are represented in **Figure 19 and 20**. It is observed that the velocity and temperature decreases with an increase of chemical reaction parameter.

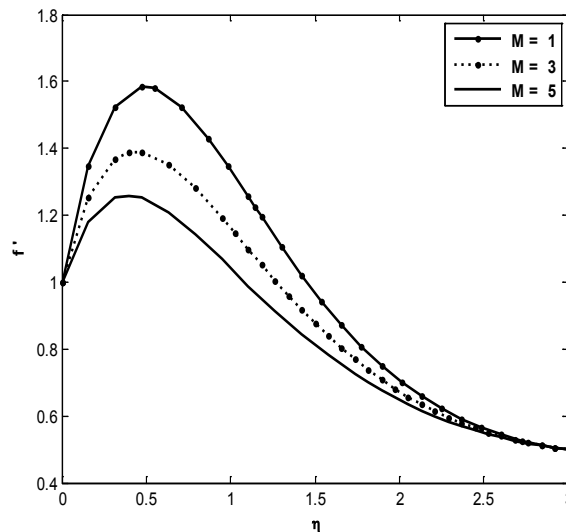


**Figure 1** Velocity profiles for different values of  $M$  when  $Pr = 0.71$ ,  $Sc = 0.60$ ,  $R = 1$ ,  $H = 0.1$ ,  $Gr = 5 = Gc$ ,  $s = 0$ ,  $c = 0.5$ ,  $K = 0.1$ ,  $K_r = 0.5$ .

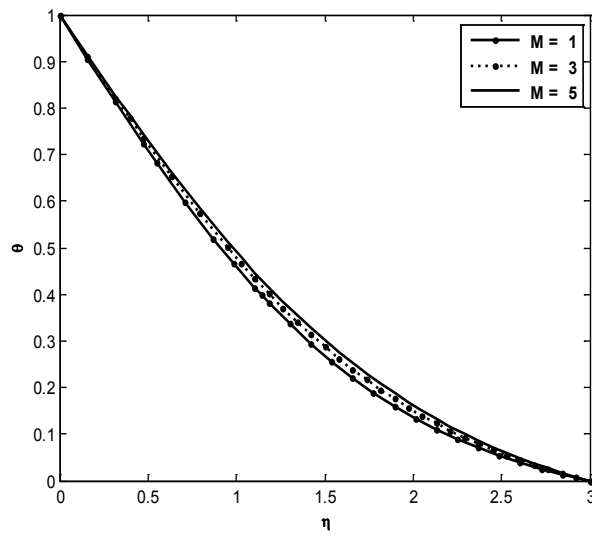


**Figure 2** Temperature profiles for different values of  $M$  when  $Pr = 0.71$ ,  $Sc = 0.60$ ,  $R = 1$ ,  $H = 0.1$ ,  $Gr = 5 = Gc$ ,  $s = 0$ ,  $c = 0.5$ ,  $K = 0.1$ ,  $K_l = 0.5$ .

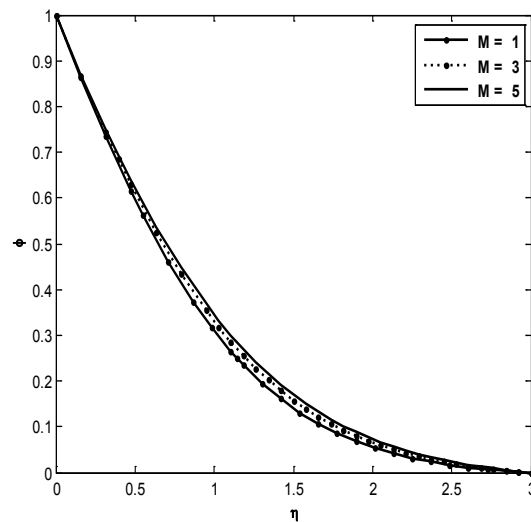


**Figure 3** Concentration profiles for different values of  $M$  when  $Pr = 0.71$ ,  $Sc = 0.60$ ,  $R = 1$ ,  $H = 0.1$ ,  $Gr = 5 = Gc$ ,  $s = 0$ ,  $c = 0.5$ ,  $K = 0.1$ ,  $K_l = 0.5$ .

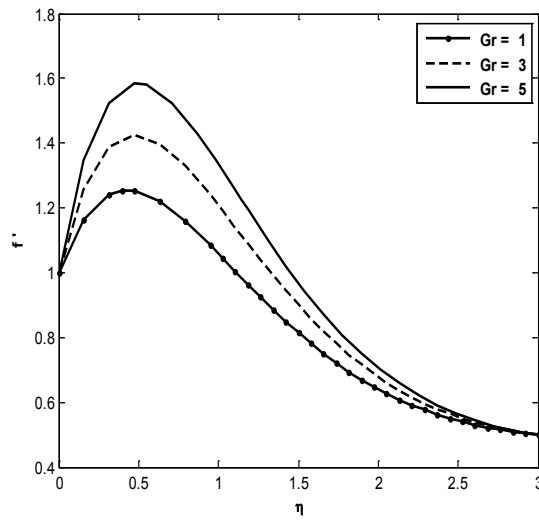


**Figure 4** Velocity profiles for different values of Gr when  $Pr = 0.71$ ,  $Sc = 0.60$ ,  $R = 1 = M$ ,  $H = 0.1$ ,  $Gc = 5$ ,  $s = 0$ ,  $c = 0.5$ ,  $K = 0.1$ ,  $K_f = 0.5$ .

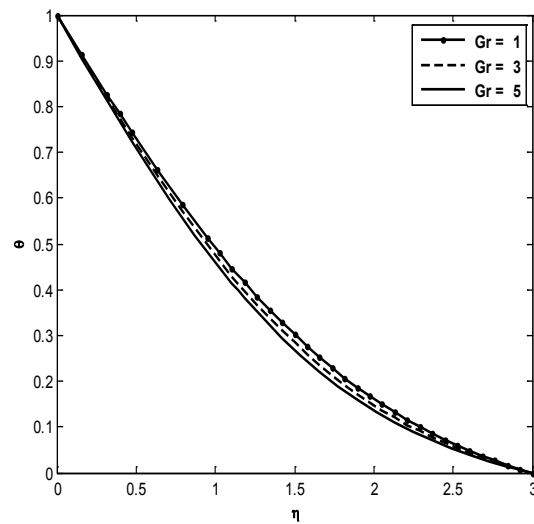


**Figure 5** Temperature profiles for different values of Gr when  $Pr = 0.71$ ,  $Sc = 0.60$ ,  $R = 1 = M$ ,  $H = 0.1$ ,  $Gc = 5$ ,  $s = 0$ ,  $c = 0.5$ ,  $K = 0.1$ ,  $K_f = 0.5$ .



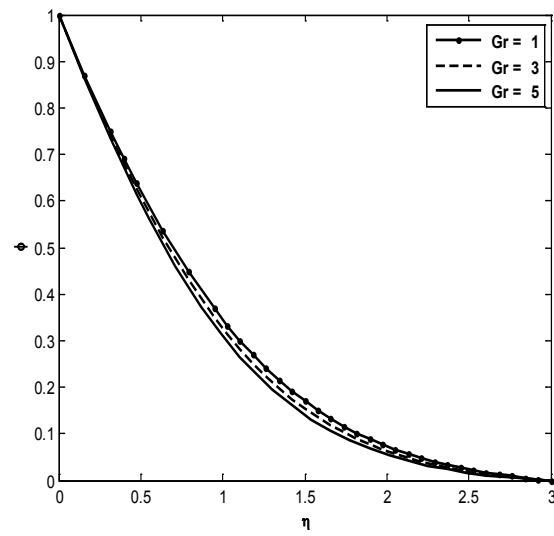


**Figure 6** Concentration profiles for different values of Gr when Pr = 0.71, Sc = 0.60, R = 1 = M, H = 0.1, Gc = 5, s = 0, c = 0.5, K = 0.1,  $K_t = 0.5$ .

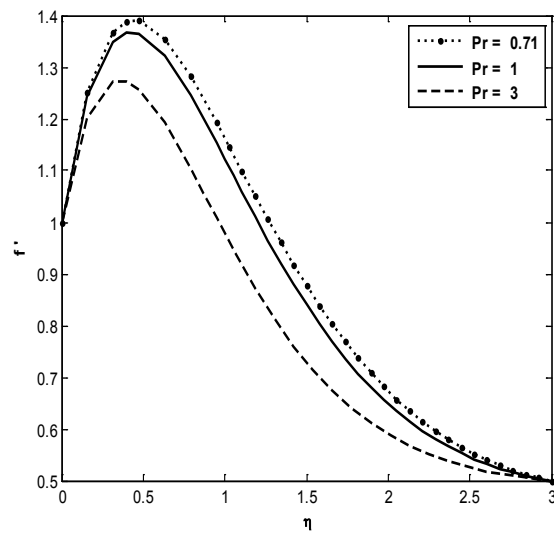


**Figure 7** Velocity profiles for different values of Pr when Sc = 0.60, R = 1 = M, H = 0.1, Gr = 5 = Gc, s = 0, c = 0.5, K = 1,  $K_t = 0.5$ .

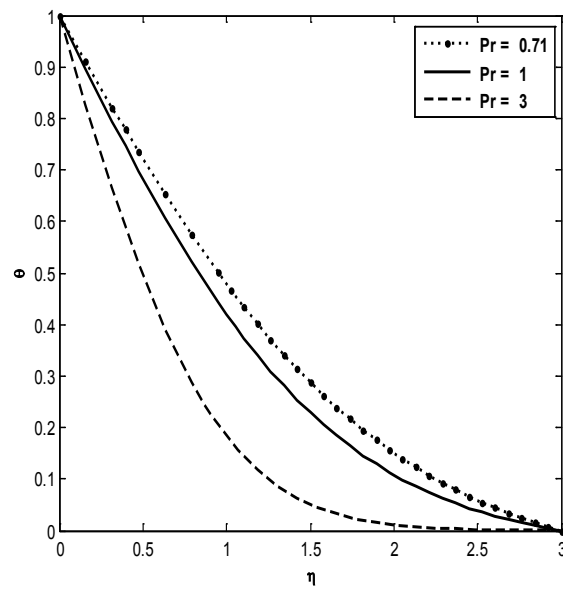


**Figure 8** Temperature profiles for different values of Pr when  $Sc = 0.60$ ,  $R = 1 = M$ ,  $H = 0.1$ ,  $Gr = 5 = Gc$ ,  $s = 0$ ,  $c = 0.5$ ,  $K = 1$ ,  $K_l = 0.5$ .

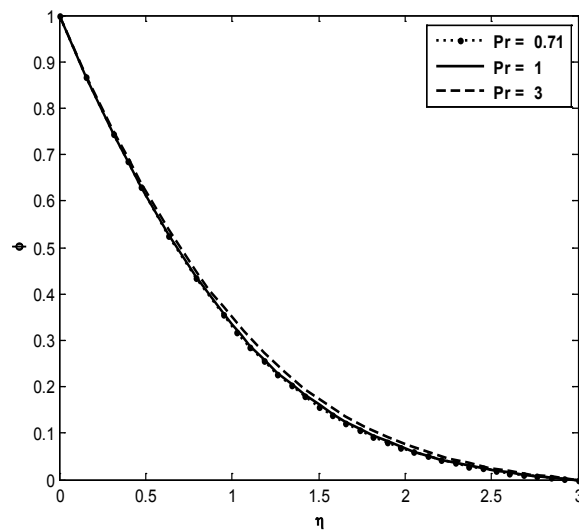


**Figure 9** Concentration profiles for different values of Pr when  $Sc = 0.60$ ,  $R = 1 = M$ ,  $H = 0.1$ ,  $Gr = 5 = Gc$ ,  $s = 0$ ,  $c = 0.5$ ,  $K = 0.1$ ,  $K_l = 0.5$ .

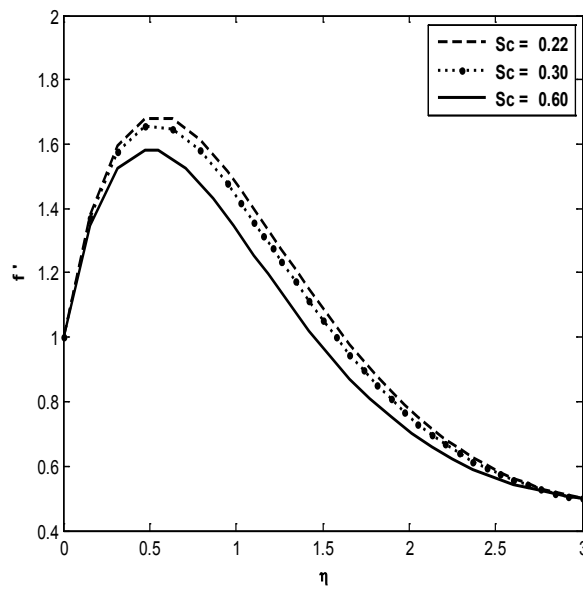


**Figure 10** Velocity profiles for different values of  $Sc$  when  $Pr = 0.71$ ,  $R = 1 = M$ ,  $H = 0.1$ ,  $Gr = 5 = Gc$ ,  $s = 0$ ,  $c = 0.5$ ,  $K = 0.1$ ,  $K_l = 0.5$ .

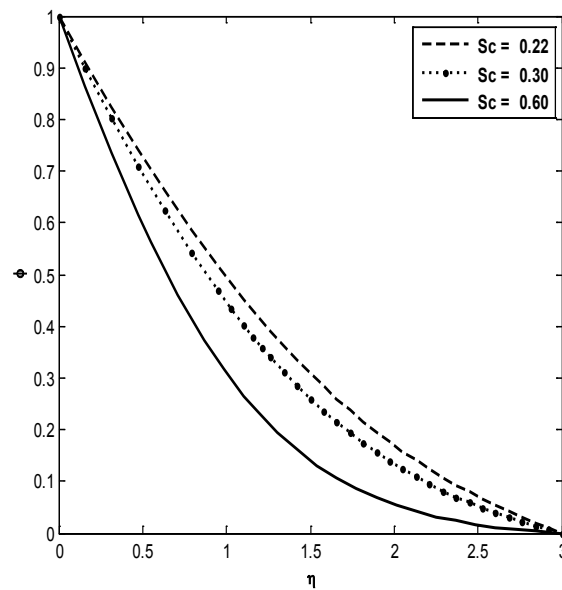


**Figure 11** Concentration profiles for different values of  $Sc$  when  $Pr = 0.71$ ,  $R = 1 = M$ ,  $H = 0.1$ ,  $Gr = 5 = Gc$ ,  $s = 0$ ,  $c = 0.5$ ,  $K = 0.1$ ,  $K_l = 0.5$ .

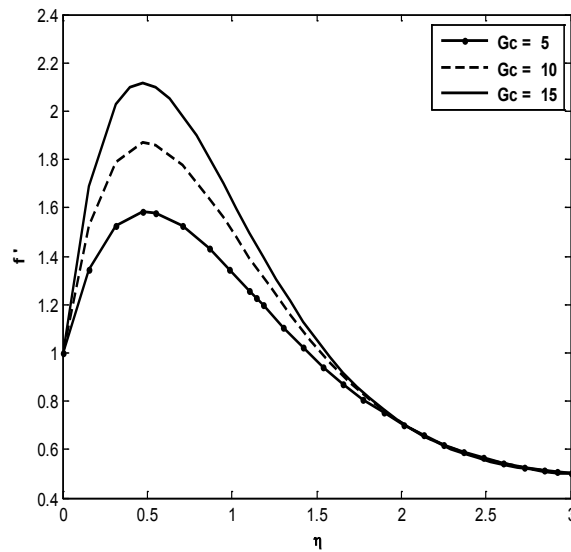


**Figure 12** Velocity profiles for different values of  $Gc$  when  $Pr = 0.71$ ,  $Sc = 0.60$ ,  $R = 1 = M$ ,  $H = 0.1$ ,  $Gr = 5$ ,  $s = 0$ ,  $c = 0.5$ ,  $K = 0.1$ ,  $K_l = 0.5$ .

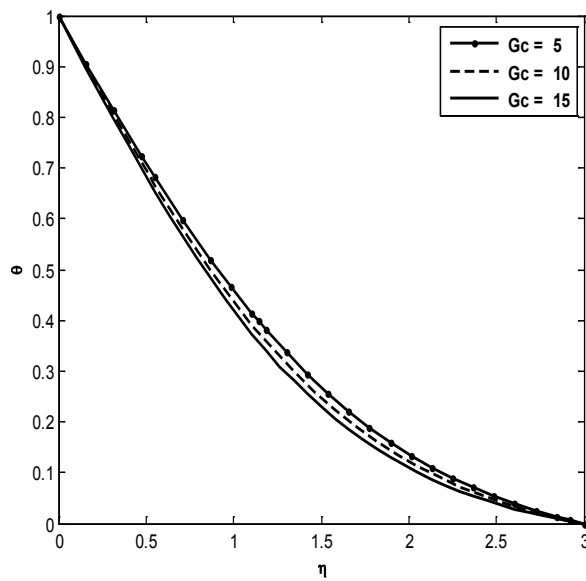


**Figure 13** Temperature profiles for different values of  $Gc$  when  $Pr = 0.71$ ,  $Sc = 0.60$ ,  $R = 1 = M$ ,  $H = 0.1$ ,  $Gr = 5$ ,  $s = 0$ ,  $c = 0.5$ ,  $K = 0.1$ ,  $K_l = 0.5$ .

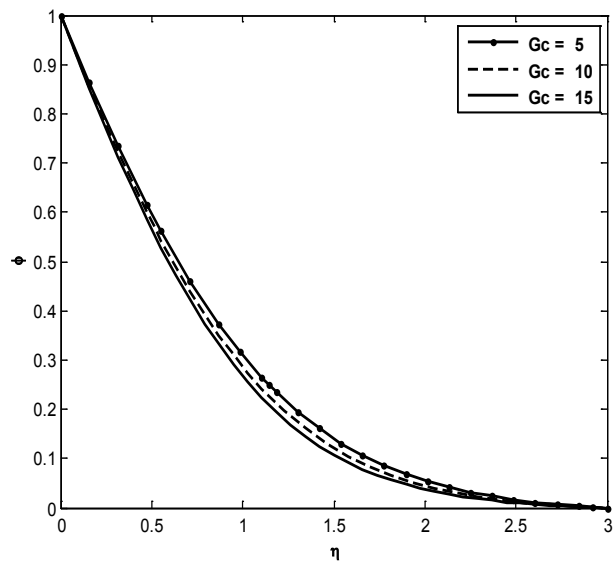


**Figure 14** Concentration profiles for different values of  $G_c$  when  $Pr = 0.71$ ,  $Sc = 0.60$ ,  $R = 1 = M$ ,  $H = 0.1$ ,  $Gr = 5$ ,  $s = 0$ ,  $c = 0.5$ ,  $K = 0.1$ ,  $K_I = 0.5$ .

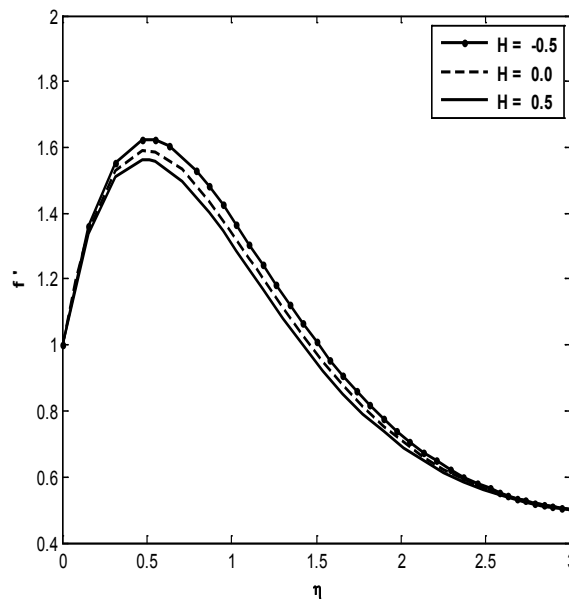


**Figure 15** Velocity profiles for different values of  $H$  when  $Pr = 0.71$ ,  $Sc = 0.60$ ,  $R = 1 = M$ ,  $Gr = 5 = G_c$ ,  $s = 0$ ,  $c = 0.5$ ,  $K = 0.1$ ,  $K_I = 0.5$ .

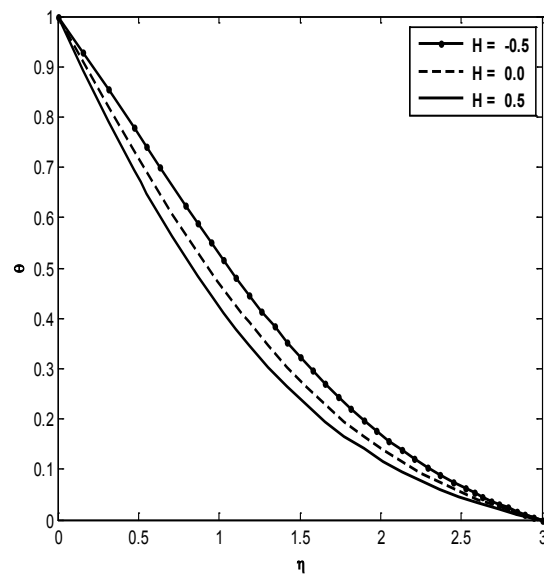


**Figure 16** Temperature profiles for different values of  $H$  when  $Pr = 0.71$ ,  $Sc = 0.60$ ,  $R = 1 = M$ ,  $Gr = 5 = Gc$ ,  $s = 0$ ,  $c = 0.5$ ,  $K = 0.1$ ,  $K_l = 0.5$ .

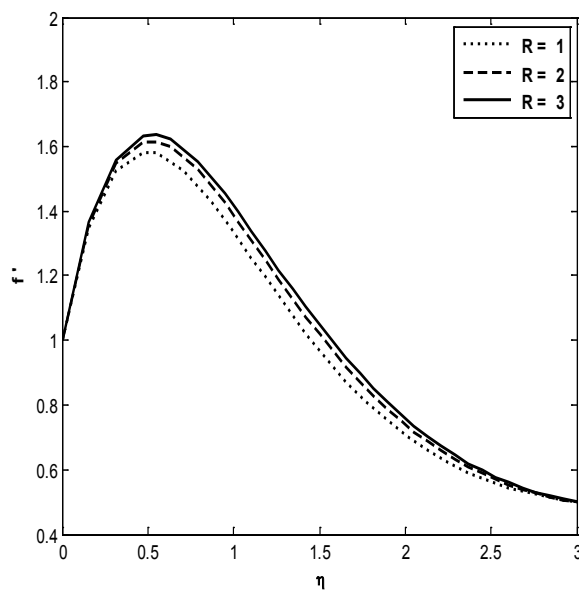


**Figure 17** Velocity profiles for different values of  $R$  when  $Pr = 0.71$ ,  $Sc = 0.60$ ,  $M = 1$ ,  $H = 0.1$ ,  $Gr = 5 = Gc$ ,  $s = 0$ ,  $c = 0.5$ ,  $K = 0.1$ ,  $K_l = 0.5$ .

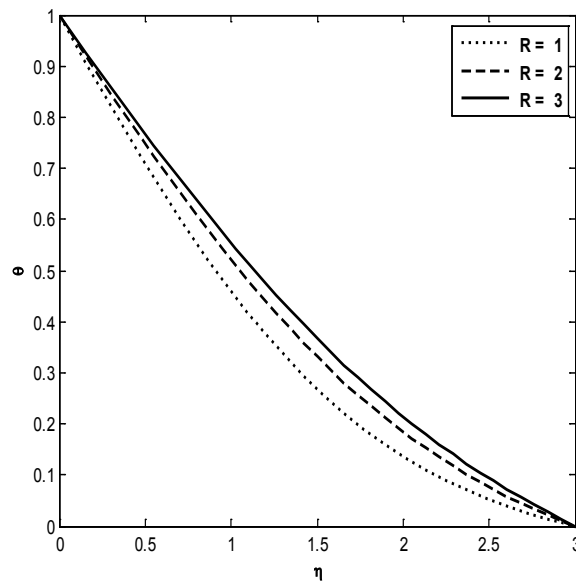


**Figure 18** Temperature profiles for different values of  $R$  when  $Pr = 0.71$ ,  $Sc = 0.60$ ,  $M = 1$ ,  $H = 0.1$ ,  $Gr = 5 = Gc$ ,  $s = 0$ ,  $c = 0.5$ ,  $K = 0.1$ ,  $K_l = 0.5$ .

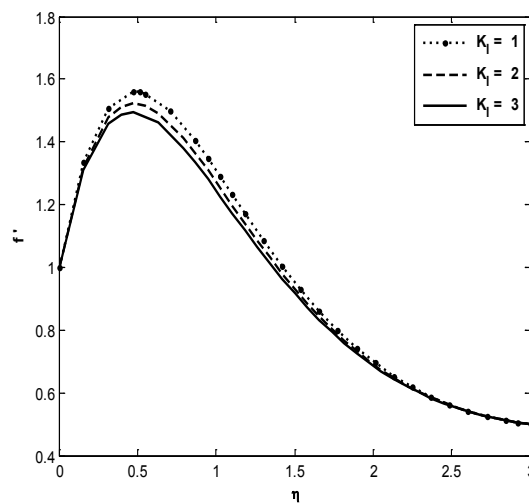


**Figure 19** Velocity profiles for different values of  $K_l$  when  $Pr = 0.71$ ,  $Sc = 0.60$ ,  $R = 1 = M$ ,  $H = 0.1$ ,  $Gr = 5 = Gc$ ,  $s = 0$ ,  $c = 0.5$ ,  $K = 1$ .

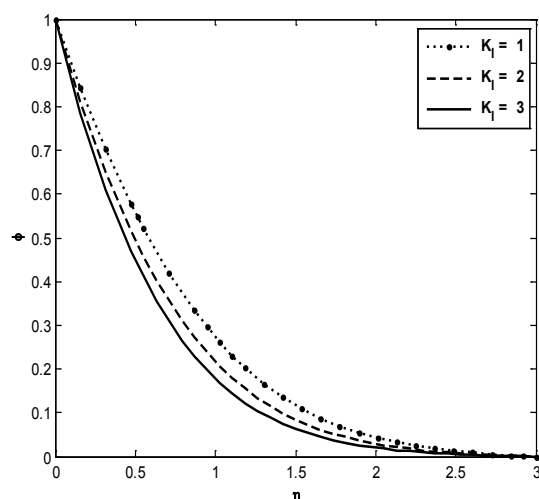


**Figure 20** Temperature profiles for different values of  $K_l$  when  $Pr = 0.71$ ,  $Sc = 0.60$ ,  $R = 1 = M$ ,  $Gr = 5 = Gc$ ,  $s = 0$ ,  $c = 0.5$ ,  $K = 0.1$ ,  $H = 0.1$ .

**Table 1** Numerical values of the skin-friction coefficients, Nusselt number, and Sherwood number for  $M$ ,  $Gr$ ,  $Gc$ ,  $R$ ,  $K$ ,  $Pr$ ,  $Sc$ ,  $H$  and  $K_l$ .

$M$	$Gr$	$Gc$	$R$	$K$	$K_l$	$Pr$	$Sc$	$H$	$f''(0)$	$-\theta'(0)$	$-\phi'(0)$
1	5	5	1	0.1	0.5	0.71	0.60	0.1	2.822002	0.598466	0.893764
2	5	5	1	0.1	0.5	0.71	0.60	0.1	2.455826	0.585918	0.878371
1	2	5	1	0.1	0.5	0.71	0.60	0.1	1.754859	0.569495	0.857645
1	5	2	1	0.1	0.5	0.71	0.60	0.1	1.877252	0.577093	0.866419
1	5	5	2	0.1	0.5	0.71	0.60	0.1	2.896710	0.516127	0.899442
1	5	5	1	0.2	0.5	0.71	0.60	0.1	2.782790	0.597110	0.892107
1	5	5	1	0.1	1	0.71	0.60	0.1	2.757986	0.595474	1.036747
1	5	5	1	0.1	0.5	3	0.60	0.1	2.057517	0.614722	0.680205
1	5	5	1	0.1	0.5	0.71	0.78	0.1	2.744508	0.594185	1.013157
1	5	5	1	0.1	0.5	0.71	0.60	0.5	2.768160	0.693130	0.890332

**Conclusions**

In this paper, we study the effects of radiation and chemical reaction on MHD convective flow over a permeable stretching surface, with suction and heat generation. The expressions for the velocity, temperature, and concentration distributions are numerically solved by using the shooting technique.

- 1) Velocity increases with the increase of  $Gr$ ,  $Gc$  and radiation parameter.
- 2) Velocity decreases with the increase of  $M$ ,  $Pr$ ,  $Sc$ ,  $H$  and  $K$ .
- 3) Skin friction, Nusselt number, and Sherwood number decreases with the increase of  $M$ ,  $Gr$ ,  $Gc$  and  $k'$ .



## References

- [1] N Sandeep and V Sugunamma. Unsteady hydromagnetic free convection flow of a dissipative and fluid past a vertical plate through porous media with constant heat flux. *Int. J. Math. Comput. Appl. Res.* 2011; **1**, 37-50.
- [2] PS Gupta and AS Gupta. Heat and mass transfer in a stretching problem with constant surface temperature. *Can. J. Chem. Eng.* 1977; **55**, 744-6.
- [3] VM Soundalgekar. Stokes problem for a viscoelastic fluid. *Acta* 1974; **13**, 177-9.
- [4] V Sugunamma, P Mohan Krishna, N Sandeep and G Vidyasagar. Radiation effect due to natural convection flow between heated inclined plates under the influence of transverse magnetic field. *Int. J. Math. Arch.* 2011; **2**, 2336-46.
- [5] N Sandeep and V Sugunamma. Effect of magnetic field due to natural convection between heated inclined plates through porous media. *Int. J. Adv. Sci. Tech. Res.* 2011; **2**, 457-69.
- [6] JH Rao, DR Jeng and KJ de Witt. Arbitrary injection/suction at a moving wall in a power-law fluid. *Int. J. Heat Mass Tran.* 1999; **42**, 2837-47.
- [7] LJ Crane and Z Angew. Flow past a stretching plate. *J. Math. Phys.* 1970; **21**, 645-7.
- [8] BC Sakiadis. Boundary-layer behavior on continuous solid surfaces, Boundary-layer equations for the two dimensional and axisymmetric flow. *AIChE J.* 1961; **7**, 26-8.
- [9] BC Sakiadis. Boundary-layer behavior on continuous solid surfaces, Boundary-layer on a continuous flat surface. *AIChE J.* 1961; **7**, 221-5.
- [10] CK Chen, MI Char and JW Cleaver. Temperature field in non-Newtonian flow over a stretching plate. *J. Math. Anal. Appl.* 1990; **151**, 301-7.
- [11] BK Dutta, P Roy and AS Gupta. Temperature field in the flow over a stretching surface with uniform heat flux. *Int. Comm. Heat Mass Tran.* 1985; **12**, 89-94.
- [12] S Bhattacharyya, A Pal and AS Gupta. Heat transfer in the flow of a viscoelastic fluid over a stretching surface. *Heat Mass Tran.* 1998; **38**, 41-5.
- [13] RS Rivlin and JL Erickson. Stress deformation relation for isotropic materials. *J. Ration. Mech. Anal.* 1955; **4**, 323-425.
- [14] NM Bujurke, SN Biradar and PS Hiremath. Second-order fluid flow past a stretching sheet with heat transfer. *Math. Phys.* 1987; **38**, 653-7.
- [15] V Sugunamma, N Sandeep, PM Krishna and R Bahunadam. Inclined magnetic field and chemical reaction effects on the flow on the semi infinite vertical porous plate through porous medium. *Comm. Appl. Sci.* 2013; **1**, 1-24.
- [16] N Sandeep and V Sugunamma. Effect of inclined magnetic field on unsteady free convection flow of dusty viscous fluid between two infinite flat plates filled by a porous medium. *Int. J. Appl. Math. Model.* 2013; **1**, 16-33.
- [17] T Hayat, Z Abbas and M Sajid. MHD stagnation-point flow of an upper-convected Maxwell fluid over a stretching surface. *Chaos Solition. Fract.* 2009; **39**, 840-8.
- [18] HI Anderson and BS Dandapat. Flow of a power-law fluid over a stretching sheet. *Stab. Appl. Anal. Cont. Media Italy* 1991; **1**, 339-47.
- [19] B Siddappa and S Abel. Non-Newtonian flow past a stretching plate. *Z. Angew. Math. Phys.* 1985; **36**, 890-2.
- [20] MI Char and CK Chen. Temperature field in non-Newtonian flow over a stretching plate with variable heat flux. *Int. J. Heat Mass Tran.* 1988; **31**, 917-21.